The EMBO Journal (2005) 24, 2306–2317 | © 2005 European Molecular Biology Organization | All Rights Reserved 0261-4189/05
www.embojournal.org

THE EMBO JOURNAL

Trafficking of STEVOR to the Maurer's clefts in *Plasmodium falciparum*-infected erythrocytes

Jude M Przyborski[1], Susanne K Miller[2], Judith M Pfahler[1], Philipp P Henrich[1], Petra Rohrbach[1], Brendan S Crabb[2] and Michael Lanzer[1,*]

[1]Hygiene Institut, Abteilung Parasitologie, Universitätsklinikum Heidelberg, Heidelberg, Germany and [2]The Walter & Eliza Hall Institute of Medical Research, Parkville, VIC, Australia

The human malarial parasite *Plasmodium falciparum* exports proteins to destinations within its host erythrocyte, including cytosol, surface and membranous profiles of parasite origin termed Maurer's clefts. Although several of these exported proteins are determinants of pathology and virulence, the mechanisms and trafficking signals underpinning protein export are largely uncharacterized—particularly for exported transmembrane proteins. Here, we have investigated the signals mediating trafficking of STEVOR, a family of transmembrane proteins located at the Maurer's clefts and believed to play a role in antigenic variation. Our data show that, apart from a signal sequence, a minimum of two addition signals are required. This includes a host cell targeting signal for export to the host erythrocyte and a transmembrane domain for final sorting to Maurer's clefts. Biochemical studies indicate that STEVOR traverses the secretory pathway as an integral membrane protein. Our data suggest general principles for transport of transmembrane proteins to the Maurer's clefts and provide new insights into protein sorting and trafficking processes in *P. falciparum*.
The EMBO Journal (2005) **24,** 2306–2317. doi:10.1038/sj.emboj.7600720; Published online 16 June 2005
Subject Categories: membranes & transport; microbiology & pathogens
Keywords: malaria; protein export; trafficking signal; transmembrane protein

Introduction

The human malarial parasite *Plasmodium falciparum* is responsible for several hundred million clinical cases, and 2–3 million deaths annually, putting a huge economic burden upon the affected countries, not to mention the suffering the infected individuals endure (World Health Organization, 2000). The high morbidity and mortality associated with falciparum malaria relate to the intraerythrocytic stages of the parasite (Miller *et al*, 2002). During asexual development within human erythrocytes, *P. falciparum* radically changes its host cell. Electron dense structures, termed knobs, appear underneath the plasma membrane of the infected erythrocyte (Kilejian, 1979) and membranous networks, extending from the parasitophorous vacuolar membrane (PVM) toward the erythrocyte periphery, fill the host cell cytoplasm (Haldar *et al*, 2002; Wickert *et al*, 2003b, 2004). Concomitantly, infected erythrocytes acquire adhesive properties and sequester in the deep vascular bed of inner organs, resulting in a broad spectrum of pathology ranging from localized hypoxia to inflammatory reactions and the syndromes of cerebral and maternal malaria (Miller *et al*, 2002).

To change the morphological and functional properties of its host erythrocyte, the parasite exports proteins into the host cell cytosol, and beyond to the erythrocyte plasma membrane. For example, the knob-associated histidine-rich protein (KAHRP), a major constituent of knobs (Culvenor *et al*, 1987; Pologe *et al*, 1987), is secreted into the erythrocyte cytoplasm to form a structure that anchors parasite-encoded immunovariant adhesins to the erythrocyte cytoskeleton (Crabb *et al*, 1997; Waller *et al*, 1999, 2002). Other exported proteins such as the skeletal binding protein 1 (PfSBP1) (Blisnick *et al*, 2000), exported protein 1 (PfEXP1) (Kara *et al*, 1988; Gunther *et al*, 1991), subtelomeric variable open reading frame (STEVOR) (Cheng *et al*, 1998; Kaviratne *et al*, 2002) and *P. falciparum* homologues of COPII proteins (Albano *et al*, 1999; Adisa *et al*, 2001; Wickert *et al*, 2003a) are associated with the membranous network or regions thereof close to the erythrocyte plasma membrane, referred to as Maurer's clefts.

The mechanisms underpinning protein transport to defined destinations within the host erythrocyte have remained largely enigmatic, despite its uniqueness. As the erythrocyte is denucleated, it consequently lacks the secretory apparatus present in eukaryotic cells. Thus, the parasite is forced to create its own protein transport machinery outside its plasma membrane. The generation of an 'extracellular' secretory system poses a challenge not met by any other organism studied thus far.

Previous studies have suggested that entry into the parasite's default secretory pathway (bulk flow), probably via the endoplasmic reticulum (ER), is mediated by a canonical (Waller *et al*, 2000; Burghaus and Lingelbach, 2001) or an unconventional N-terminal signal sequence (Wickham *et al*, 2001). The default pathway allows trafficking of proteins across the parasite's plasma membrane to the lumen of the parasitophorous vacuole (Wickham *et al*, 2001; Lopez-Estrano *et al*, 2003). Recent studies have identified a recessed host cell targeting (HCT) signal, which appears to be conserved in a large number of predicted secreted proteins, for transport across the PVM (Hiller *et al*, 2004; Marti *et al*, 2004). Interestingly, the same HCT signal appears to play a role in the export of both soluble and transmembrane proteins (Hiller *et al*, 2004; Marti *et al*, 2004), suggesting that, for integral membrane proteins, there must be additional

*Corresponding author. Hygiene Institut, Abteilung Parasitologie, Universitätsklinikum Heidelberg, Im Neuenheimer Feld 324, 69120 Heidelberg, Germany. Tel.: +49 6221 567845; Fax: +49 6221 564643; E-mail: michael_lanzer@med.uni-heidelberg.de

Received: 1 December 2004; accepted: 27 May 2005; published online: 16 June 2005

sequence elements mediating their sorting to parasite-derived membrane profiles within the host erythrocyte cytoplasm, such as the Maurer's clefts.

As a model for integral membrane proteins targeted to the Maurer's clefts, we have studied trafficking of STEVOR. First reported as 7h8 (Limpaiboon *et al*, 1991), STEVOR proteins are encoded by a subtelomerically located multigene family composed of 30–40 members, dependent on parasite strain (Blythe *et al*, 2004), and represent, together with the erythrocyte surface located RIFINS, a large superfamily of variant antigens (Cheng *et al*, 1998). STEVOR variants are 30–40 kDa in size and are predicted to contain a signal sequence and two transmembrane domains flanking a hypervariable loop region (Cheng *et al*, 1998; Sam-Yellowe *et al*, 2004). A similar domain structure has been reported for RIFIN and PfMC-2TM (Sam-Yellowe *et al*, 2004).

Transcription of *stevor* in asexual stages occurs within a tight developmental window 22–32 h after invasion, with peak transcription coinciding with the mid-trophozoite stage (Kaviratne *et al*, 2002). Single parasites transcribe more than one *stevor*; however, only a subset of *stevor* is transcribed at any given time in cultured parasites (Kaviratne *et al*, 2002). From the trophozoite stage on, STEVOR can be localized to the Maurer's clefts (Kaviratne *et al*, 2002). STEVOR is also expressed in gametocytes and sporozoites, suggesting that it fulfills a function at different time points throughout the parasite life cycle (McRobert *et al*, 2004). The small size of STEVOR and its transmembranous nature make it an amenable and relevant tool with which to study export and trafficking of integral membrane proteins in *P. falciparum*-infected erythrocytes. Our data show that trafficking of STEVOR to the Maurer's clefts is a complex process requiring multiple signals.

Results

A full-length STEVOR-GFP fusion protein is targeted to Maurer's clefts

Initially, we examined targeting of full-length STEVOR fused to the green fluorescent protein (GFP) (STEVOR^{full}). Confocal laser scanning microscopy of parasites expressing STEVOR^{full} revealed a dotted fluorescence pattern within the host erythrocyte cytoplasm, characteristic of the Maurer's clefts (Figure 1A). A control parasite line expressing GFP alone revealed a fluorescence signal confined within the boundaries of the parasite plasma membrane (Figure 1A). To verify a localization of STEVOR^{full} to Maurer's clefts, we performed immunofluorescence colocalization studies using antisera recognizing the established Maurer's clefts marker PfSBP1 (Blisnick *et al*, 2000) as well as PfEMP1 (Wickert *et al*, 2003b), which transiently associates with Maurer's clefts on its way to the erythrocyte plasma membrane (Wickham *et al*, 2001; Kriek *et al*, 2003; Wickert *et al*, 2003b). Both PfSBP1 and PfEMP1 colocalize with the chimeric STEVOR^{full} protein (Figure 1B), consistent with previous studies (Kaviratne *et al*, 2002). These data indicate that a full-length STEVOR-GFP fusion protein, unlike GFP alone, is exported from the parasite and properly targeted to the Maurer's clefts, suggesting that all signals necessary for transport are contained within the STEVOR primary sequence.

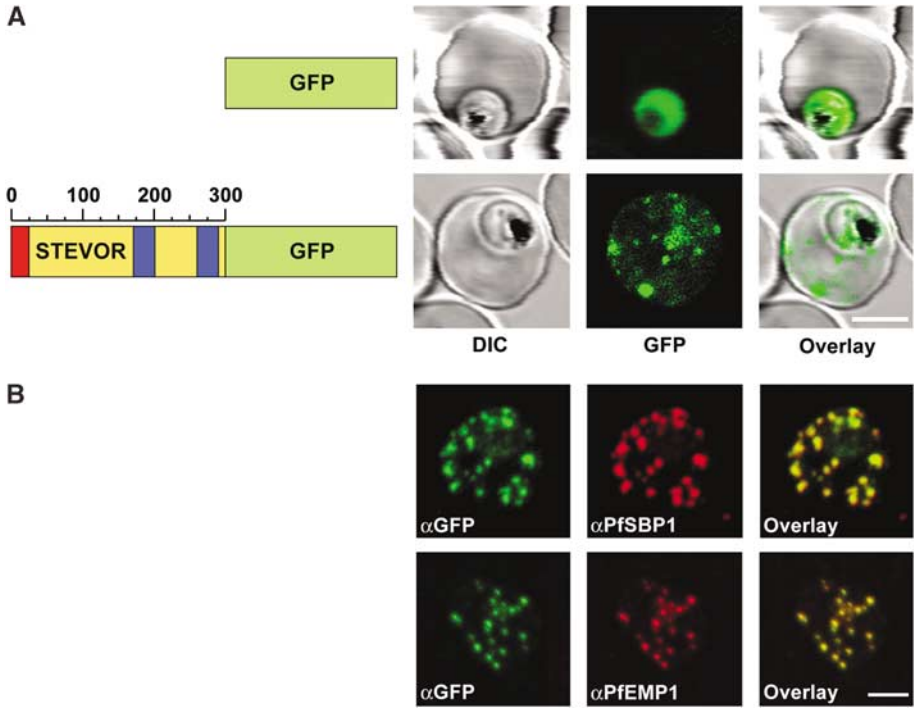

Figure 1 Subcellular localization of STEVOR^{full} and GFP in *P. falciparum*-infected erythrocytes. (**A**) The upper row represents control (GFP alone) and the lower row STEVOR^{full}. The left image shows differential interference contrast (DIC), middle image GFP fluorescence and the right image overlay. The GFP-only control reveals fluorescence only within the boundaries of the parasite plasma membrane. STEVOR^{full} exhibits a dotted fluorescence pattern within the host erythrocyte cytoplasm, characteristic of the Maurer's clefts. Scale refers to the residue number of STEVOR. Red, signal sequence; blue, predicted transmembrane domains; yellow, bulk of STEVOR; green, GFP. Bar, 4 μm. (**B**) Colocalization of STEVOR^{full} (αGFP) with PfSBP1 (αPfSBP1) and/or PfEMP1 (αPfEMP1) by immunofluorescence microscopy. Overlay of signals is shown in the right panel. Bar, 3 μm.

An N-terminal signal sequence and a recessed host cell targeting signal are necessary for STEVOR export into the erythrocyte cytosol

To investigate signals mediating targeting of STEVOR to the Maurer's clefts, we generated C-terminal nested deletions. Transfectant lines expressing up to and including the first 20 amino acids of STEVOR exhibit patterns of fluorescence identical to the GFP-only control line, with the fluorescence signals confined within the body of the parasite (Figure 2). Upon adding a further 5 amino acids, the fluorescence signal changed significantly, with the chimera being exported to the lumen of the parasitophorous vacuole. Consistent with this interpretation, we occasionally observed fluorescent protrusions of the PVM. These data indicate that the first 25 amino acids of STEVOR constitute a functional signal sequence, which allows entry into the secretory system and export across the parasite plasma membrane into the parasitophorous vacuole.

We next created further lines expressing the first 35, 40, 45, 50, 60, 70 and 80 N-terminal amino acids of STEVOR fused to GFP. All transfectant lines expressing up to and including the first 60 amino acids of the STEVOR N-terminal region show a pattern of fluorescence indistinguishable from that of STEVOR$^{1-25}$, that is, GFP fluorescence is confined to the lumen of the parasitophorous vacuole and only little fluorescence is seen within the parasite body (Figure 2). No fluorescence is evident within the host erythrocyte cytosol (Figure 2).

The addition of a further 10 amino acids (STEVOR$^{1-70}$) changes the distribution of the fluorescence signal. Now, a population of the chimeric protein is transported to the cytosol of the erythrocyte, as is evident by the diffuse fluorescence pattern throughout the entire erythrocyte cytosol (Figure 2). Fluorescence can also be seen within a ring structure surrounding the body of the parasite, corresponding to the lumen of the parasitophorous vacuole, and within the

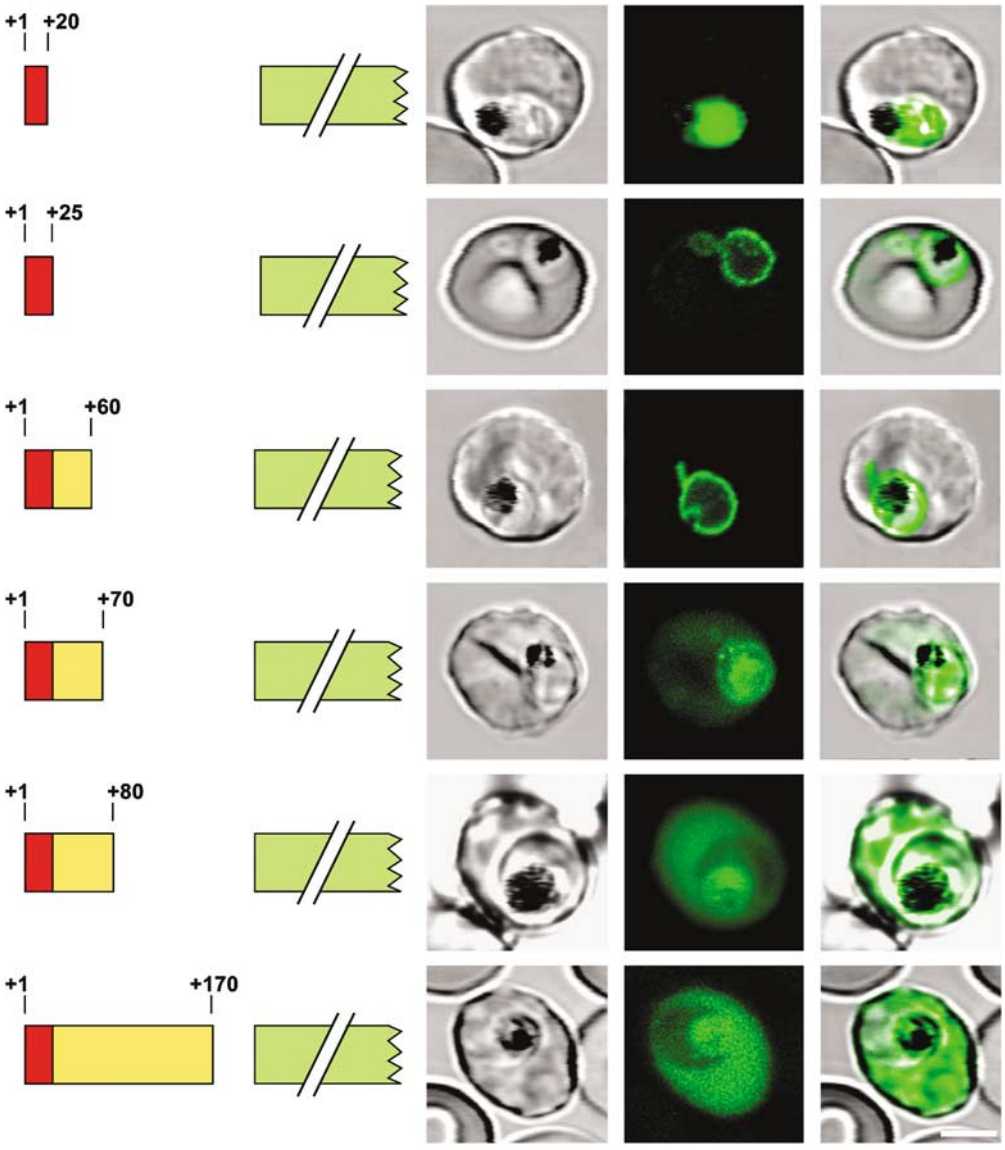

Figure 2 Nested deletional analysis of STEVOR. The confocal images show the subcellular localization of different STEVOR-GFP chimera in *P. falciparum*-infected erythrocytes: STEVOR$^{1-20}$ (top row), STEVOR$^{1-25}$ (second row), STEVOR$^{1-60}$ (third row), STEVOR$^{1-70}$ (fourth row), STEVOR$^{1-80}$ (fifth row) and STEVOR$^{1-170}$ (bottom row). Parasites exporting soluble chimera to the parasitophorous vacuole frequently display fluorescent protrusions of the PVM. The predicted signal sequence of STEVOR is shown in red (left side). Green, GFP. Bar, 4 μm.

parasite's body, including the large food vacuole (Figure 2). Food vacuolar GFP fluorescence is commonly seen in transfectant lines exporting fluorescent chimera to the host cell cytosol (Waller *et al*, 2000; Wickham *et al*, 2001), and has been interpreted as resulting from the uptake of the erythrocyte cytosol by the parasite during feeding. The fluorescence signal within the erythrocyte cytosol substantially increased when the STEVOR N-terminal sequence was extended to include the first 80 amino acids (Figure 2). No further changes in the fluorescence patterns were observed in transfectant lines expressing the first 170 amino acids of STEVOR fused to GFP (Figure 2).

To further delineate the first 80 N-terminal amino acids of STEVOR, we deleted amino acids 26–50, which contain conserved HCT motifs (Figure 3A) (Hiller *et al*, 2004; Marti *et al*, 2004). The resulting chimera STEVOR$^{\Delta 26-50}$ remained confined to the parasitophorous vacuole (Figure 3B). We next mutated within the HCT motif residues K^{46}, R^{48} and Q^{52}. Interestingly, all three mutants revealed different phenotypes. Replacing Q^{52} by an alanine completely abrogated export into the host erythrocyte, with the chimeric protein accumulating in the parasitophorous vacuolar lumen (Figure 4). In mutant R^{48}A, export into the host erythrocyte was also blocked; however, the mutated protein remained in the parasite with some of the protein being found in a perinuclear compartment indicative of the ER (Figure 4). In the case of mutant K^{46}A, the protein was exported to the host erythrocyte cytoplasm, yet some of it accumulated in the ER (Figure 4).

We further mutated charged amino acids surrounding the HCT motif. Charged amino acids have been implicated in protein trafficking to organelles, including chloroplast mitochondria and apicoplast (Neupert and Brunner, 2002; Foth *et al*, 2003; Soll and Schleiff, 2004). Mutants R^{42}A and R^{34}A showed a phenotype similar to that of mutant K^{46}A, that is, export of the protein into erythrocyte host cytosol and accumulation of some protein in the ER (Figure 4). Replacing H^{59}, H^{61}, D^{63}, E^{65}, K^{67}, E^{68}, D^{71}, K^{72}, E^{75}, D^{76}, K^{79} or K^{80} by an alanine had no effect on protein export into the host erythrocyte (Figure 4 and data not shown). The apparent indifference of residues downstream of the HCT motif seemed to contrast with the subcellular localization of STEVOR$^{1-60}$, which remained in the parasitophorous vacuole in spite of a complete HCT motif (see Figure 2 for comparison). We therefore wondered whether downstream sequences may only be necessary to spatially separate the HCT motif from the GFP reporter. Indeed, adding an alanine linker immediately following amino acid 60 or 70 (yielding STEVOR^{1-69A} and STEVOR^{1-70A}) now resulted in complete export of the chimeric proteins to the erythrocyte cytosol (Figure 5), confirming that sequences following amino acid 60 play no specific role in export of STEVOR to the host erythrocyte cytosol.

Further transport of STEVOR to the Maurer's clefts is mediated by a transmembrane domain

Inclusion of the first 217 amino acids of STEVOR, which contain a predicted transmembrane domain (amino acids 178–194), drastically changes the distribution of the fluorescence signal within the host cell. In transfectants expressing STEVOR$^{1-217}$, discreet foci of fluorescence are observed within the erythrocyte cytoplasm, characteristic of a Maurer's clefts localization (Figure 6A). Extending the STEVOR-GFP fusion protein to include the first 260 amino acids showed a fluorescence pattern identical to STEVOR$^{1-217}$ (Figure 6A).

These data suggest that targeting of STEVOR to the Maurer's clefts requires a minimum of three distinct signals: an N-terminal signal sequence, a recessed HCT signal and

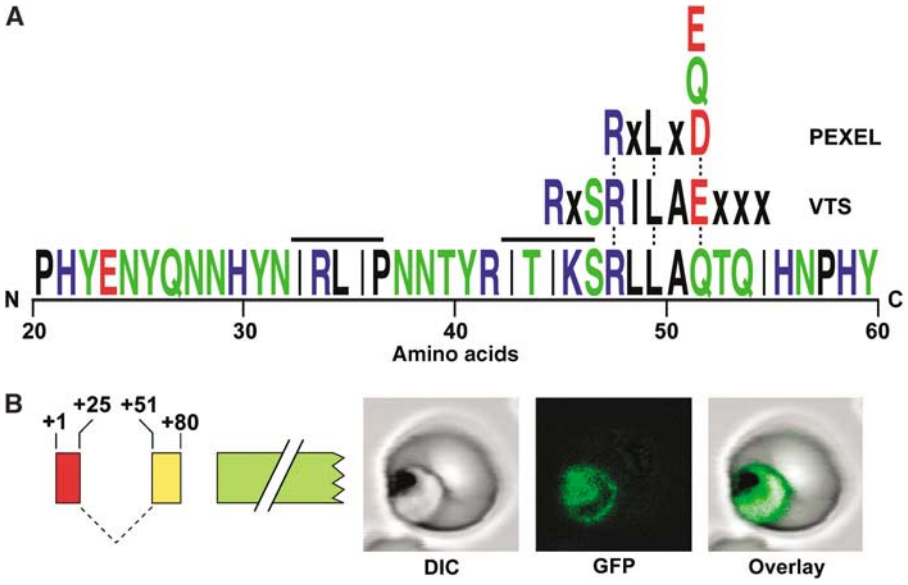

Figure 3 Dissecting the HCT signal of STEVOR. (**A**) An alignment of the first 21–60 amino acids of STEVOR with the PEXEL (*Plasmodium* export element) (Marti *et al*, 2004) and the VTS (vacuolar transport signal) (Hiller *et al*, 2004). Predicted chaperone binding sites are indicated by an upper bar (see Supplementary Figure S1). The color code for amino acids is as follows: black, hydrophobic; blue, acidic; green, polar; red, basic. (**B**) Subcellular localization of STEVOR$^{\Delta 26-50}$ in *P. falciparum*-infected erythrocytes. In this chimera, the signal sequence of STEVOR (red, amino acids 1–25) was fused to amino acids 51–80, thereby deleting amino acids 26–50 (dotted line). The fluorescence signal is largely retained in a ring structure surrounding the body of the parasite, corresponding to the lumen of the parasitophorous vacuole. Fluorescence is also detected in the parasite's food vacuole. Left image, DIC; middle image, GFP; right image, overlay. Bar, 4 μm.

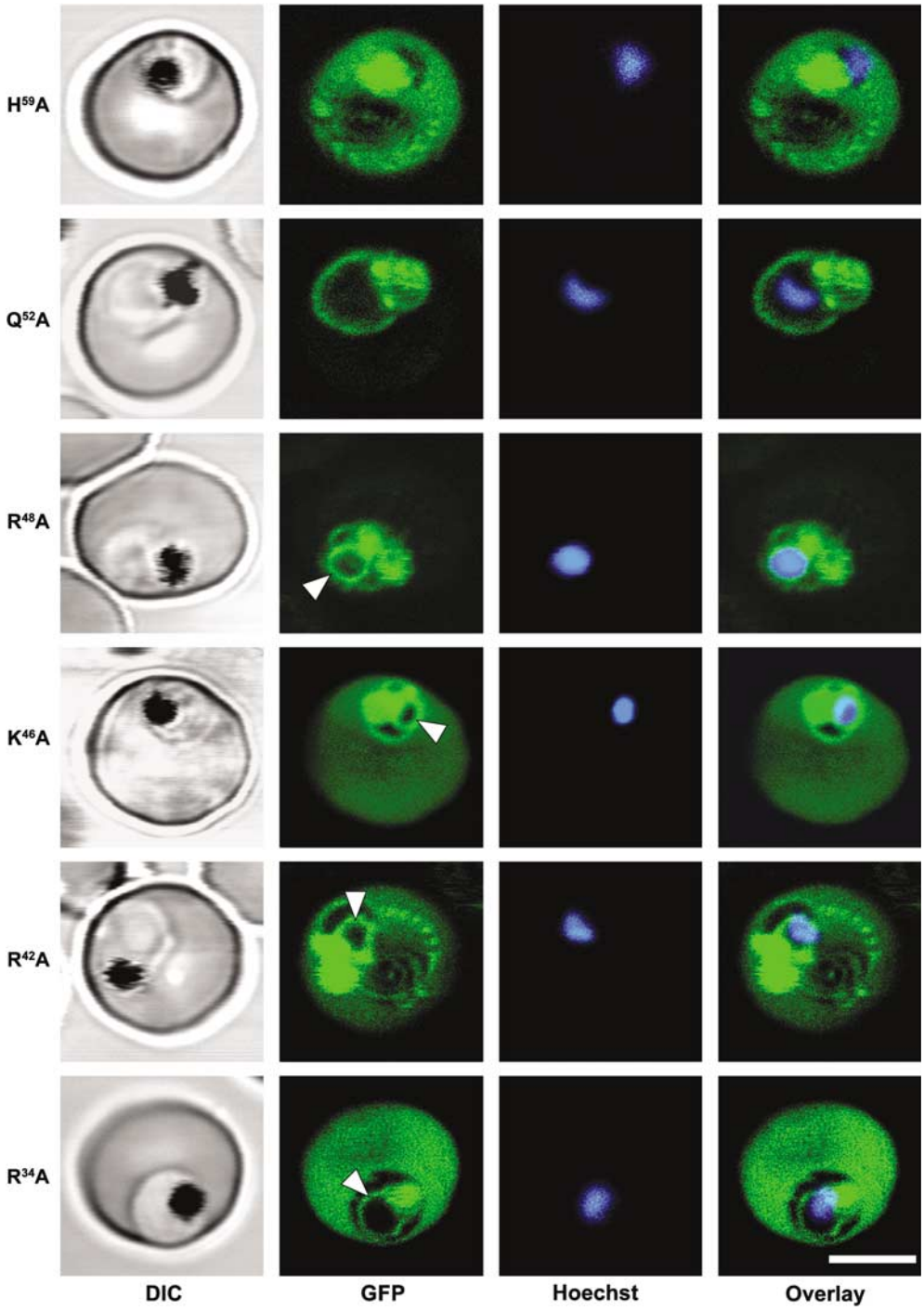

Figure 4 Mutational analysis of the STEVOR HCT signal. Residues in superscript were replaced by an alanine and the subcellular localizations of the resulting GFP chimera (derived from $STEVOR^{1-80}$) were detected by confocal fluorescence microscopy. $H^{59}A$ revealed fluorescence in the host erythrocyte cytoplasm. In the case of $Q^{52}A$, the fluorescence signal is largely retained in a ring structure surrounding the body of the parasite, corresponding to the lumen of the parasitophorous vacuole. Mutant $R^{48}A$ revealed fluorescence in the parasite including the ER (indicated by an arrow). Mutants $K^{46}A$, $R^{42}A$ and $R^{34}A$ showed fluorescence in the host erythrocyte cytoplasm and in a perinuclear compartment (indicated by an arrow). First column, DIC; second column, GFP; third column, nuclear staining with Hoechst; fourth column, overlay of green and blue channels. Bar, 4 μm.

a transmembrane domain. To verify this, we generated two minimal constructs containing the first 80 amino acids of STEVOR, followed by either the first or second STEVOR transmembrane domain, fused to GFP ($STEVOR^{TM1}$ and $STEVOR^{TM2}$). In both cases, the chimeric proteins are targeted to the Maurer's clefts (Figure 6B), as verified by immunofluorescence colocalization with PfSBP1 (Figure 6C).

STEVOR enters the secretory system at the ER as an integral membrane protein

To investigate whether STEVOR traffics via the ER, we fused $STEVOR^{1-80}$ to the ER retention signal KDEL (Figure 7A). In the resulting transfectant line ($STEVOR^{1-80KDEL}$), a distinct ring of fluorescence surrounding the parasite's nucleus is observed, consistent with an ER localization (Figure 7A).

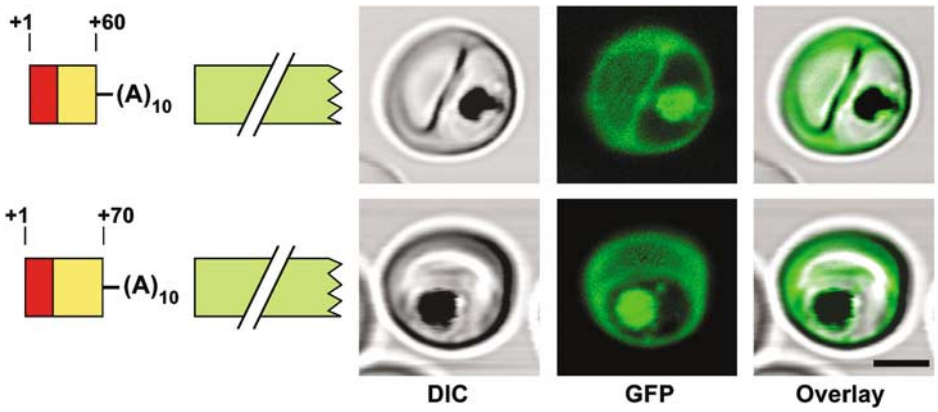

Figure 5 Spatial requirements between the HCT signal and the GFP reporter. A 10-residue alanine linker was added between the STEVOR sequences at the residue indicated and the GFP reporter. The subcellular localizations of the resulting chimera are shown by confocal fluorescence microscopy. Compare the subcellular localization of STEVOR^{1-60A} with that of STEVOR$^{1-60}$ in Figure 2. Left image, DIC; middle image, GFP; right image, overlay. Bar, 4 μm.

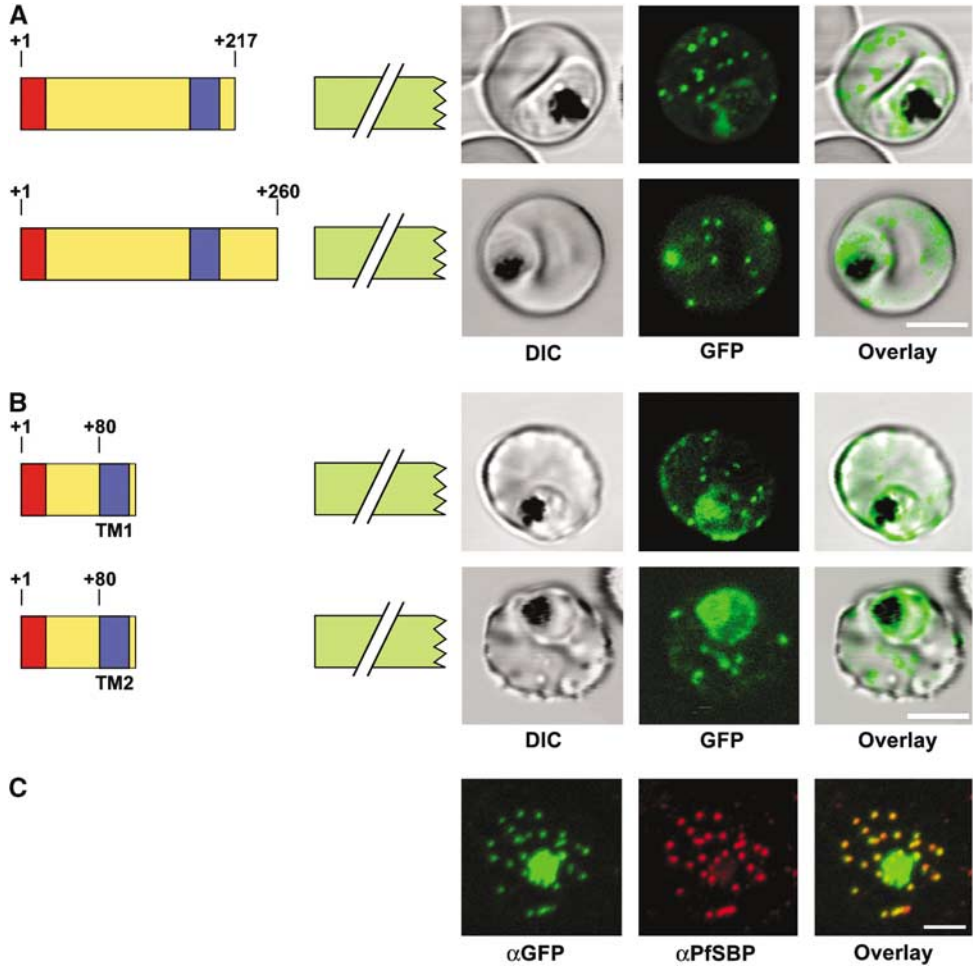

Figure 6 Effect of a transmembrane domain on targeting of STEVOR to the Maurer's clefts. (**A**) Subcellular localization of STEVOR$^{1-217}$ and STEVOR$^{1-260}$. A punctuate GFP fluorescence is observed within the cytosol of the host erythrocyte, consistent with a Maurer's clefts localization. Left image, DIC; middle image, GFP; right image, overlay. Bar, 4 μm. (**B**) Subcellular localization of the minimal functional chimera STEVOR^{TM1} (top row) and STEVOR^{TM2} (lower row). These chimera are composed of the first 80 N-terminal amino acids of STEVOR including the signal sequence (red) fused to either the first or second STEVOR transmembrane domain (blue) and the associated charged residues. A punctuate GFP fluorescence is observed within the cytosol of the host erythrocyte, consistent with a localization in Maurer's clefts. Some fluorescence is also noted associated with the parasite. (**C**) Colocalization of STEVOR^{TM1} (αGFP) and PfSBP1 (αPfSBP1) by immunofluorescence microscopy. Bar, 3 μm.

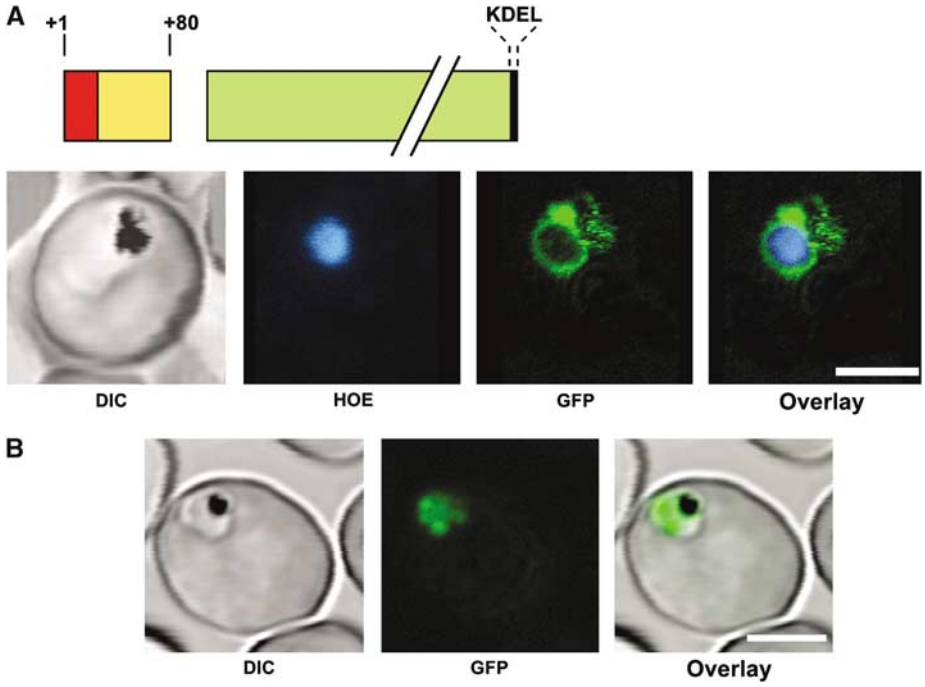

Figure 7 Analysis of the intraparasitic trafficking pathway of STEVOR. (**A**) Subcellular localization of STEVOR$^{1-80KDEL}$ containing the ER retention signal KDEL. Fluorescence is confined to a perinuclear compartment corresponding to the parasitic ER. First column, DIC; second column, GFP; third column, nuclear staining with Hoechst; fourth column, overlay of green and blue channels. Bar, 4 μm. (**B**) STEVOR^{full} transport is brefeldin A sensitive. Highly synchronized ring-stage parasites were treated with brefeldin A prior to observation of the GFP fluorescence signal. The STEVOR^{full} chimera accumulates within the body of the parasite, with no fluorescence being seen within the host erythrocyte cytoplasm. Bar, 4 μm.

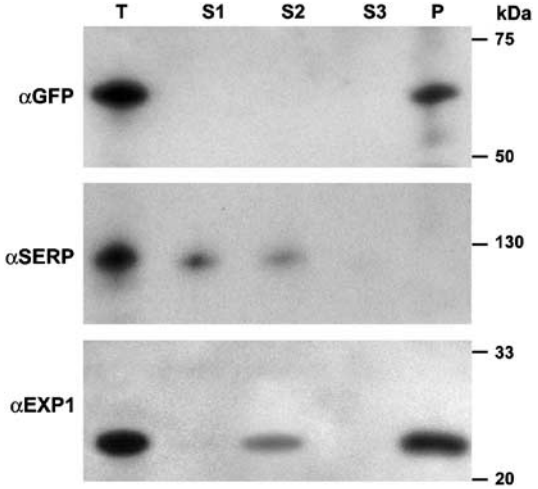

Figure 8 Extraction profile of STEVOR in the parasite's secretory pathway. Highly synchronized ring-stage parasites expressing STEVOR^{full} were treated with brefeldin A for 16 h to arrest protein export. Parasites were lysed, yielding a total lysate (T), and the membranes were separated from the supernatant (S1). The total membrane fraction was then washed with carbonate (S2) and extracted with urea (S3). The nonextractable fraction yielded the final membrane pellet (P). Extracts from 2×10^7 parasites were examined per lane by Western analysis using antibodies against GFP (αGFP recognizing STEVOR^{full}), PfSERP (αSERP) and PfEXP1 (αEXP1). Protein size standards are indicated in kDa. A representative example of three independent sets of experiments is shown.

Previous studies have shown that secretion through the ER/Golgi-mediated pathway in *P. falciparum* is sensitive to brefeldin A (Benting *et al*, 1994; Wickham *et al*, 2001). We reasoned that, if STEVOR is exported by this pathway, brefeldin A should abrogate its transport. To investigate this, highly synchronized ring-stage parasites expressing STEVOR^{full} were treated with brefeldin A for 16 h, resulting in the retention of the chimeric protein in an intraparasitic compartment (Figure 7B). This compartment is commonly seen in brefeldin A-treated parasites, and has been shown to represent the plasmodial ER (Wiser *et al*, 1997; Wickham *et al*, 2001). To investigate in which state STEVOR^{full} traverses the secretory pathway, membrane fractions from the brefeldin A-treated parasites were prepared and subjected to a carbonate wash, to remove peripheral proteins from the membrane, followed by urea extraction to differentiate between proteins anchored in the membrane by protein–protein or protein–lipid interactions (Papakrivos *et al*, 2005). A Western analysis using anti-GFP antibodies revealed a signal of the expected size of 60 kDa for STEVOR^{full} exclusively in the final membrane pellet, and not in the water-soluble supernatant, the carbonate wash or the urea extract (Figure 8), consistent with STEVOR^{full} being transported as an integral membrane protein. As controls, we investigated the soluble protein PfSERP and the integral membrane protein PfEXP1. PfSERP mainly associates with the water-soluble fraction, yet some PfSERP is also observed in the carbonate wash (Figure 8), consistent with previous data (Papakrivos *et al*, 2005). PfEXP1 is mainly found in the final membrane pellet, although some PfEXP1 is also found in the carbonate wash (Figure 8), possibly because prolonged treatment of the cells with brefeldin A resulted in improper cotranslational membrane insertion of this protein.

STEVOR^{full} in the Maurer's clefts is partly urea extractable

A previous study has indicated that PfEMP1, a family of immunovariant antigens that transiently associates with the Maurer's clefts on their way to the erythrocyte surface (Craig and Scherf, 2001), is anchored in its target membrane by protein–protein interactions, as suggested by the extractability of PfEMP1 from membranes by urea (Papakrivos *et al*, 2005). To investigate the membrane association of STEVOR at its final destination within the Maurer's clefts, we prepared total membrane fractions from parasites expressing STEVOR^{full}, which were then subjected to extraction with urea. As a control, cells expressing STEVOR$^{1-60}$ were examined in parallel. As shown in Figure 9, STEVOR^{full} is associated with the membrane pellet fraction, although a significant portion is urea extractable. In comparison, STEVOR$^{1-60}$ is found mainly in the water-soluble fraction, as was PfSERP (Figure 9). PfEMP1 was only found in the urea-soluble fraction, and human glycophorin B and PfEXP1 in the membrane pellet (Figure 9), consistent with a previous report (Papakrivos *et al*, 2005).

Membrane topology of STEVOR

To determine the topology of STEVOR in the Maurer's clefts, erythrocytes infected with parasites expressing STEVOR^{full} and STEVOR$^{1-260}$ were permeabilized with streptolysin O and then incubated with an anti-GFP antibody. In the case of STEVOR^{full}, both immunofluorescence (anti-GFP antibody) and GFP fluorescence colocalized in the Maurer's clefts (Figure 10A), suggesting that the C-terminal GFP-containing domain of the protein is exposed to the erythrocyte cytosol (Figure 10B). In comparison, the C-terminus of STEVOR$^{1-260}$, containing only one transmembrane domain, appears to lie within the lumen of the Maurer's cleft, as the GFP tail was not accessible to the anti-GFP antibody (Figure 10A and B).

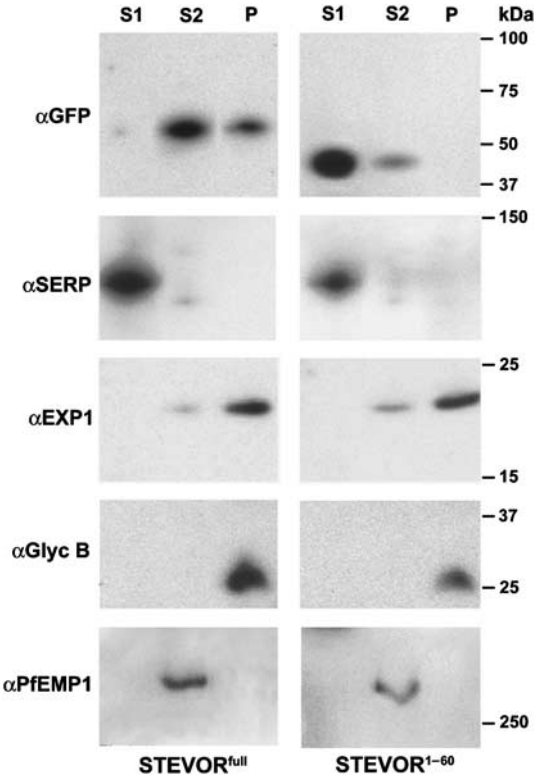

Figure 9 Extraction profile of STEVOR in the Maurer's clefts. Mature-stage infected erythrocytes expressing STEVOR^{full} or STEVOR$^{1-60}$ were lysed and the membranes separated from the supernatant (S1). The total membrane fraction was extracted with urea (S2). The nonextractable fraction yielded the final membrane pellet (P). Extracts from 2×10^7 parasites were examined per lane by Western analysis using antibodies against GFP (αGFP recognizing STEVOR^{full}), PfSERP (αSERP), PfEXP1 (αEXP1), human glycophorin B (αGlyc B) and PfEMP1 (αPfEMP1). Protein size standards are indicated in kDa. The results were verified for two independent preparations.

Discussion

Our data suggest that export of STEVOR to the *P. falciparum* Maurer's clefts is a multistep process that requires a minimum of three defined signals contained within the STEVOR primary sequence. This includes (1) an N-terminal signal sequence for entry into the secretory pathway and secretion across the parasite plasma membrane into the parasitophorous vacuole, (2) an HCT signal for passage through the PVM and entry into the host erythrocyte cytosol and (3) a transmembrane domain for sorting to the Maurer's clefts.

P. falciparum possesses an intracellular secretory machinery including an ER and a functional, albeit not morphologically defined Golgi (Elmendorf and Haldar, 1993, 1994). Our data suggest that STEVOR traffics via this pathway. Treatment of transfected parasites with brefeldin A prevented export of STEVOR^{full} from the parasite and led to retention within the ER (Figure 7A). Similarly, the addition of the lumenal ER retention signal KDEL resulted in accumulation of STEVOR$^{1-80KDEL}$ in the ER (Figure 7A).

Previous studies have suggested that entry into the *P. falciparum* secretory pathway is mediated by a signal sequence, which may be either canonical, as found in PfEXP1 (Burghaus and Lingelbach, 2001) and HRPII (Lopez-Estrano *et al*, 2003), or functional, as exemplified by KAHRP (Wickham *et al*, 2001). STEVOR contains a canonical N-terminal signal sequence. Signal sequences are usually cleaved during translocation into the lumen of the ER, as shown in other systems (Blobel and Dobberstein, 1975), and for *P. falciparum* EXP1 (Burghaus and Lingelbach, 2001) and KAHRP (Wickham *et al*, 2001). Cleavage of the STEVOR signal sequence is predicted but has to date not been experimentally verified.

N- and C-terminal deletional analysis as well as site-directed mutagenesis revealed the presence of an HCT signal contained between amino acids 26 and 60, which is required for targeting STEVOR into the host cell. This region contains the conserved RxLxE/Q/D, respectively RxSRILAExxx motif (Figure 3A), which, according to previous studies, appears to be required for protein trafficking into the host erythrocyte cytosol (Hiller *et al*, 2004; Marti *et al*, 2004). Consistent with this view, deletion of this motif from the STEVOR primary sequence or replacing key amino acids within it (R^{48}A and Q^{52}A) completely abrogates export to the host cell cytoplasm. Unexpectedly, the two mutants R^{48}A and Q^{52}A accumulate the mutated protein in different subcellular compartments. In mutant Q^{52}A, the protein is located in the lumen of the parasitophorous vacuole. In mutant R^{48}A, however, the protein is not retained in the parasitophorous vacuole but within the parasite including the ER, in spite of a functional signal sequence (Figure 4). A similar phenotype was also observed

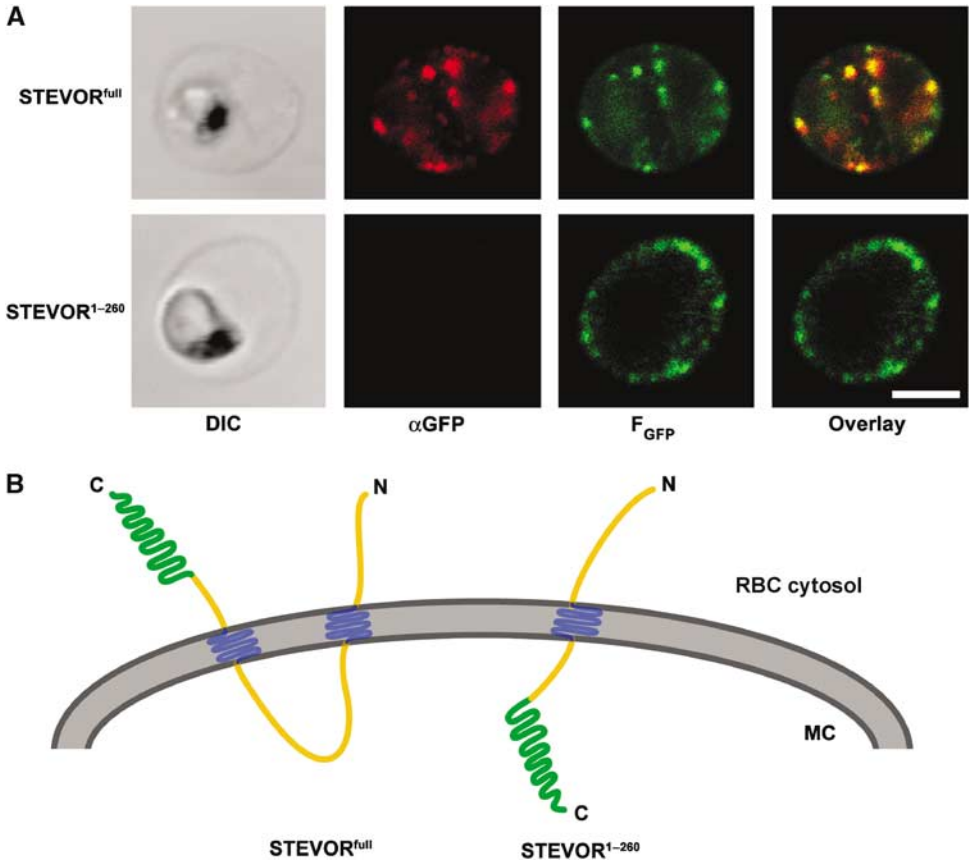

Figure 10 Membrane topology of STEVOR^{full} and STEVOR$^{1-260}$. (**A**) Erythrocytes infected with mature-stage parasites expressing STEVOR^{full} or STEVOR$^{1-260}$ were permeabilized with streptolysin O and incubated with mouse anti-GFP antibodies followed by an anti-mouse Cy2-conjugated secondary antibody. Cy2 fluorescence (αGFP) and GFP fluorescence (F_{GFP}) were observed by confocal laser scanning microscopy. Bar, 4 μM. (**B**) Model of membrane topology of STEVOR-GFP chimera in the Maurer's clefts. Green, GFP; yellow, STEVOR; blue, STEVOR transmembrane domain; RBC, red blood cell; MC, lumen of the Maurer's cleft.

by Hiller *et al* (2004) and Marti *et al* (2004) but not commented upon. At present, we can only speculate about the cause of these two different phenotypes. It may be that the HCT motif is not just required for translocation across the PVM, as previously thought (Hiller *et al*, 2004; Marti *et al*, 2004), but may also play a role in other events, such as protein stability and/or quality control in the ER.

Residues preceding the conserved HCT motif appear to play an auxiliary role during transport processes. Mutation of either amino acid K^{46}, R^{42} or R^{34} did not ablate trafficking into the host erythrocyte cytoplasm, yet resulted in a significant and clearly discernable portion of the chimeric protein being retained within the parasite's ER (see for comparison Figure 7B). Interestingly, these residues are part of predicted chaperone binding sites (Figure 3A and Supplementary Figure S1). As shown in other systems, translocation processes are often aided by molecular chaperones, which appear to prevent retrograde movement by drawing the protein across the membrane, and facilitate correct protein folding (Neupert and Brunner, 2002).

Residues beyond the conserved HCT motif do not appear to provide specific information for trafficking, as demonstrated by site-directed mutagenesis of 13 different residues between positions 56 and 80, and by bulk replacement of 10 residues by alanines following position 60. In this context, it is interesting to note the requirement for a spacer between the conserved HCT motif and the GFP reporter, as exemplified by STEVOR$^{1-60}$, which is retained in the parasitophorous vacuole despite possessing a complete HCT motif. The translocation block is overcome by the insertion of a 10-amino-acid alanine spacer between STEVOR$^{1-60}$ and GFP (see STEVOR^{1-60A}). The need for a spatial separation between the HCT motif and GFP may help explain previous data in which GFP fusion proteins failed to translocate across the PVM despite the presence of a complete HCT signal (Wickham *et al*, 2001; Lopez-Estrano *et al*, 2003).

In this study, we furthermore show that a transmembrane domain is crucial for the eventual targeting of STEVOR to the Maurer's clefts. Parasite lines expressing constructs STEVOR$^{1-217}$, STEVOR^{TM1} and STEVOR^{TM2} exhibit dotted fluorescence patterns within the host erythrocyte cytoplasm (Figure 6), identified as Maurer's clefts using antisera to the specific marker PfSBP1 (Figure 6C). Thus, the addition of a predicted transmembrane domain drastically changes the subcellular localization of the corresponding STEVOR chimera within the host erythrocyte cytosol, from an apparently diffusible soluble form to a membrane-bound state.

One can envisage two different models for transport of STEVOR to the Maurer's clefts. The first model imagines that STEVOR traverses the secretory pathway in a soluble, non-membrane-bound form, in a manner similar to that previously described for PfEMP1 (Papakrivos *et al*, 2005), and

only after passage across the PVM would STEVOR insert into parasite-derived membranes, including Maurer's clefts, by virtue of its transmembrane domains. The second model would predict that STEVOR inserts cotranslationally into the ER membrane and traverses the secretory pathway as an integral membrane protein. To differentiate between the two models, we determined the extraction and solubility profile of STEVOR^{full} after treatment of ring-stage parasites with brefeldin A for 16 h to block protein export from the ER (see Figure 8) (Benting *et al*, 1994; Wickham *et al*, 2001). Our finding that STEVOR^{full} associates with the parasite's membrane fraction, and is not found in the water-soluble fraction, the carbonate wash or the urea extract, would support a model in which STEVOR traverses the secretory pathway as an integral membrane protein. In comparison, PfEMP1 within the secretory pathway can be extracted by carbonate, and it has been suggested that PfEMP1 is translocated into the ER lumen and is secreted as a sodium carbonate-extractable protein (Papakrivos *et al*, 2005). Thus, STEVOR and PfEMP1 appear to traverse the secretory pathway differently, although both are targeted to the Maurer's clefts. On this note, the signals required for trafficking also appear to differ between these two proteins (Hiller *et al*, 2004; Marti *et al*, 2004; Przyborski and Lanzer, 2004; Knuepfer *et al*, 2005) and PfEMP1 seems to possess an atypical transmembrane domain (Papakrivos *et al*, 2005). Moreover, there appear to be proteins, including the integral membrane protein PfSBP1, that lack the conserved HCT motif, but are nevertheless targeted to the Maurer's clefts (Blisnick *et al*, 2000; Vincensini *et al*, 2005), suggesting alternative trafficking signals and possibly pathways.

At the Maurer's clefts, the extraction profile of STEVOR slightly changes (Figure 9). STEVOR still associates with the membrane fraction, but some protein can be extracted from the membrane with urea. In comparison, PfEMP1 is only found in the urea extract, which has been interpreted in terms of a model in which PfEMP1 is anchored in the membrane by protein–protein rather than protein–lipid interactions (Papakrivos *et al*, 2005). Whether STEVOR interacts with other transmembrane proteins in the Maurer's clefts is speculative, but would be consistent with its partial extractability with urea. While our study has identified a set of discreet signals necessary for trafficking of an integral membrane protein to the *P. falciparum* Maurer's clefts, the transport machinery recognizing these signals and the nature of the interactions remain elusive.

Materials and methods

In silico analysis

Multiple sequence alignments were carried out at http://www.ebi.ac.uk/clustalw/ (Thompson *et al*, 1994). Transmembrane domains were predicted using TMHMM v. 2.0 at http://www.cbs.dtu.dk/services/TMHMM-2.0 (Moller *et al*, 2001), and signal sequences using SignalP v. 3.0 (Bendtsen *et al*, 2004). Chaperone binding sites were predicted using a previously described algorithm (Rudiger *et al*, 1997).

Vector construction

Primers *stev*^{for} and *stev*^{rev} were designed to PCR amplify a full-length *stevor* gene from the *P. falciparum* clone 3D7. The resulting product was cloned into pCR2.1^{TOPO} (Invitrogen, designated pCR2.1-STEV^{full}) and individual clones sequenced using M13 F + R primers. The GFPmut2 coding sequence was amplified from plasmid pHC1-ACP$_L$ (Waller *et al*, 2000) using primers *gfp*^{Afor} and *gfp*^{Krev} and cloned into the *Avr*II/*Kpn*I restriction site of the expression vector pARL1a$^+$ (Crabb *et al*, 2004) to create pARL1-GFP. pARL-STEVOR^{full}: A fragment encoding one entire *stevor* gene but missing the stop codon was amplified from clone pCR2.1-STEVOR^{full} using primers *stev*^{Xfor} and *stev*^{Arev} and cloned into the *Xho*I/*Avr*II site of pARL1-GFP. pARL-STEVOR$^{1-5,1-10}$: Fragments encoding the first 5 or 10 amino acids of STEVOR were created by annealing complementary oligonucleotides *stev*^{5for}, *stev*^{5rev} and *stev*^{10for}, *stev*^{10rev}. These fragments were then ligated to *Xho*I/*Avr*II-restricted pARL1-GFP. pARL-STEVOR$^{1-15}$: A fragment encoding the first 15 amino acids of STEVOR was created with overlapping oligonucleotides. Primers *stev*^{15for} and *stev*^{15rev} were annealed, filled in with Klenow, digested with *Xho*I/*Avr*II and ligated to *Xho*I/*Avr*II-restricted pARL1-GFP. pARL-STEVOR$^{(1-20)-(1-260)}$: Oligonucleotide primers were designed to allow amplification of fragments encoding between 20 and 260 amino acids of STEVOR. The following primers were used together with primer *stev*^{Xfor}: *stev*^{20rev}, *stev*^{25rev}, *stev*^{30rev}, *stev*^{35rev}, *stev*^{40rev}, *stev*^{45rev}, *stev*^{50rev}, *stev*^{60rev}, *stev*^{70rev}, *stev*^{A80rev}, *stev*^{170rev}, *stev*^{217rev}, *stev*^{260rev}. Fragments were digested with *Xho*I/*Avr*II and ligated to *Xho*I/*Avr*II-digested pARL1-GFP. pARL2-STEVOR$^{1-25,51-80}$: A linker derived from annealed complementary oligonucleotides *pl*^{for} and *pl*^{rev} was cloned into *Xho*I/*Xma*I-digested pARL1a$^+$ to create pARL2. GFPmut2 coding sequence was amplified from pARL1-GFP with primers *gfp*^{Kfor} and *gfp*^{Xrev} and cloned into *Kpn*I/*Xma*I-digested pARL2 to create pARL2-GFP. A fragment encoding amino acids 51–80 of STEVOR was obtained by PCR from template pARL-STEVOR^{full} with primers *stev*^{51for} and *stev*^{K80rev}. A fragment encoding the first 25 amino acids of STEVOR was obtained by *Xho*I/*Avr*II digestion of pARL-STEVOR$^{1-25}$ and was used in a three-part ligation with *Avr*II/*Kpn*I-restricted fragment *stev*$^{51-80}$ to *Xho*I/*Kpn*I-digested pARL2-GFP to create pARL2-STEVOR$^{\Delta 26-50}$. pARL2-STEVOR$^{TM1/TM2}$: A fragment encoding STEVOR amino acids 26–80 was amplified with from template pARL-STEVOR^{full} with primer pair *stev*^{26for} and *stev*^{K80rev}. A further fragment encoding either the first or the second TM domain of STEVOR was amplified from template pARL-STEVOR^{full} using primer combinations *stev*^{tm1for}, *stev*^{tm1rev} and *stev*^{tm2for}, *stev*^{tm2rev}. The fragment encoding either TM1 or TM2 was then used in a three-part ligation reaction together with fragment *stev*$^{26-80}$ from above to *Avr*II/*Kpn*I-digested pARL2$^-$STEVOR$^{\Delta 26-50}$. pARL-STEV$^{1-80KDEL}$: A fragment was amplified from template pARL-STEVOR$^{1-80}$ with primers *stev*^{Xfor} and *gfp*^{KDELrev} and cloned into *Xho*I/*Kpn*I-restricted pARL1a+. pARL-STEVOR$^{1-60A,1-70A}$: A polylinker was created by annealing oligos 10A^{for}/10A^{rev}. Fragments encoding STEVOR$^{1-60,1-70}$ were obtained by *Xho*I/*Avr*II digestion of pARL-STEVOR$^{1-60/1-70}$, and were then used in a three-piece ligation with the polylinker to *Xho*I/*Kpn*I-restricted pARL2-GFP to give pARL-STEVOR$^{1-60A,1-70A}$. All constructs were checked by restriction digest and automated sequencing.

Site-directed mutagenesis

A fragment encoding STEVOR$^{26-80}$ was amplified from template pARL-STEVOR^{full} using primer pair stev^{BA25for} and stev^{K80rev}, digested with *Xba*I/*Kpn*I and cloned into pGEM7Zf (Promega) to create pGEM$^{26-80}$. Site-directed mutagenenesis was carried out using the GeneTailor kit (Invitrogen) and pGEM$^{25-80}$ as template. Fragments containing the required mutations were then released by digestion with *Avr*II/*Kpn*I and cloned into *Avr*II/*Kpn*I-restricted pARL-STEVOR$^{\Delta 26-50}$. All constructs were checked by restriction digest and automated sequencing.

Parasite culture and transfection

The *P. falciparum* clone 3D7 was cultured in 0$^+$ human erythrocytes as described previously (Trager and Jensen, 1976) in RPMI media supplemented with 5% 0$^+$ human serum, 0.25% Albumax II (Gibco), 200 μM hypoxanthine and 20 μg/ml gentamycin. Cultures were synchronized by sorbitol lysis (Lambros and Vanderberg, 1979). Parasites were transfected with 100 μg plasmid DNA and transfectants selected with 5 nm WR99210 as described previously (Fidock and Wellems, 1997). Resistant parasites were first seen in blood smears between days 13 and 50.

Brefeldin A treatment

Treatment of highly synchronized ring-stage parasites with 5 μg/ml brefeldin A (Sigma) was carried out as described previously (Wickham *et al*, 2001).

Indirect immunofluorescence assay

Immunofluorescence was carried out on air-dried monolayers as described previously (Haeggstrom *et al*, 2004). Primary antisera and dilutions were as follows: guinea-pig anti-PfEMP1 1:200 (Wickert *et al*, 2003b), rabbit anti-GFP 1:200 (Clontech), mouse anti-PfSBP1 1:100 (gift of C Braun-Breton). Corresponding secondary antibodies conjugated to either Alexa 488 or 546 were used at a dilution of 1:800. Slides were mounted with mowiol and viewed using an LSM510 laser scanning confocal microscope (Carl Zeiss, Jena). Parasites at the trophozoite stage were investigated.

Membrane preparation and protein analysis

Soluble, carbonate, urea and membrane protein fractions were prepared as described previously (Papakrivos *et al*, 2005). Samples corresponding to 2×10^7 parasites/lane were separated on NuPage gels (Invitrogen) and transferred to PVDF as recommended by the manufacturer. Membranes were then probed with α-EXP1, α-SERP, α-glycophorin (gifts of Klaus Lingelbach) and α-ExonII antisera as described previously (Wickert *et al*, 2003b; Papakrivos *et al*, 2005). Mouse anti-GFP antibodies (Roche) were used at 1:200, PBS/5% skimmed milk, for 2 h at room temperature (RT), followed by 30 min horseradish peroxidase-conjugated goat anti-mouse (Dianova, 1:20 000, PBS/5% skimmed milk). Membranes were developed using the Supersignal Femto kit (Pierce), and exposed to Kodak BioMax XAR film.

Labelling of internal GFP populations

Trophozoite-stage parasites expressing either $STEVOR^{full}$ or $STEVOR^{1-60}$ were purified on a MACS column as described previously (Staalsoe *et al*, 1999). The purified infected erythrocytes were permeabilized with streptolysin O (a gift from Klaus Lingelbach) as described previously (Ansorge *et al*, 1996), and incubated with mouse anti-GFP antibodies (Roche, 1:200, PBS/2% FCS, 1 h RT) followed by a Cy2-conjugated donkey anti-mouse secondary antibody (Dianova, 1:1000, PBS/2% FCS, 1 h RT). Parasites were viewed at RT on an LSM510 laser scanning confocal microscope (Carl Zeiss) at the appropriate wavelengths.

Confocal microscopy and image processing

P. falciparum-infected erythrocytes were viewed within 20 min of removal from culture at RT in phenol red free RPMI media in a perfusion chamber on an LSM510 confocal laser scanning microscope (Carl Zeiss, Jena). GFPmut2 and fusion protein derivatives were excited at 488 nm using an argon laser (Argon, laser power 40%, transmission 2%, C-Apochromat ×63/1.2 water immersion). Throughout the study, we examined parasites at the trophozoite stage, and the data shown are representative of at least 20 independent observations.

Online supplemental material

Primers and oligonucleotides used in this study are compiled in Supplementary Table S1. Supplementary Figure S1 shows prediction of chaperone binding sites within STEVOR.

Supplementary data

Supplementary data are available at *The EMBO Journal* Online.

Acknowledgements

This work was supported by a grant from the Deutsche Forschungsgemeinschaft (La 941/7-1) and the European Commission (BioMalPar). We thank Catherine Braun-Breton for anti-PfSBP1 antibodies, Tim Gilberger for the transfection vector pARL1a$^+$ and Klaus Lingelbach for anti-PfEXP1, anti-PfSERP, anti-human glycophorin B and streptolysin O. WR99210 was a gift from D Jacobus, Jacobus Pharmaceuticals, Princeton, NJ. We are grateful to Klaus Lingelbach and Stefan Charpian for helpful and stimulating discussions.

References

Adisa A, Albano FR, Reeder J, Foley M, Tilley L (2001) Evidence for a role for a *Plasmodium falciparum* homologue of Sec31p in the export of proteins to the surface of malaria parasite-infected erythrocytes. *J Cell Sci* **114:** 3377–3386

Albano FR, Berman A, La Greca N, Hibbs AR, Wickham M, Foley M, Tilley L (1999) A homologue of Sar1p localises to a novel trafficking pathway in malaria-infected erythrocytes. *Eur J Cell Biol* **78:** 453–462

Ansorge I, Benting J, Bhakdi S, Lingelbach K (1996) Protein sorting in *Plasmodium falciparum*-infected red blood cells permeabilized with the pore-forming protein streptolysin O. *Biochem J* **315:** 307–314

Bendtsen JD, Nielsen H, von Heijne G, Brunak S (2004) Improved prediction of signal peptides: SignalP 3.0. *J Mol Biol* **340:** 783–795

Benting J, Mattei D, Lingelbach K (1994) Brefeldin A inhibits transport of the glycophorin-binding protein from *Plasmodium falciparum* into the host erythrocyte. *Biochem J* **300** (Part 3)**:** 821–826

Blisnick T, Morales Betoulle ME, Barale JC, Uzureau P, Berry L, Desroses S, Fujioka H, Mattei D, Braun Breton C (2000) Pfsbp1, a Maurer's cleft *Plasmodium falciparum* protein, is associated with the erythrocyte skeleton. *Mol Biochem Parasitol* **111:** 107–121

Blobel G, Dobberstein B (1975) Transfer of proteins across membranes. I. Presence of proteolytically processed and unprocessed nascent immunoglobulin light chains on membrane-bound ribosomes of murine myeloma. *J Cell Biol* **67:** 835–851

Blythe JE, Surentheran T, Preiser PR (2004) STEVOR—a multifunctional protein? *Mol Biochem Parasitol* **134:** 11–15

Burghaus PA, Lingelbach K (2001) Luciferase, when fused to an N-terminal signal peptide, is secreted from transfected *Plasmodium falciparum* and transported to the cytosol of infected erythrocytes. *J Biol Chem* **276:** 26838–26845

Cheng Q, Cloonan N, Fischer K, Thompson J, Waine G, Lanzer M, Saul A (1998) *stevor* and *rif* are *Plasmodium falciparum* multicopy gene families which potentially encode variant antigens. *Mol Biochem Parasitol* **97:** 161–176

Crabb BS, Cooke BM, Reeder JC, Waller RF, Caruana SR, Davern KM, Wickham ME, Brown GV, Coppel RL, Cowman AF (1997) Targeted gene disruption shows that knobs enable malaria-infected red cells to cytoadhere under physiological shear stress. *Cell* **89:** 287–296

Crabb BS, Rug M, Gilberger TW, Thompson JK, Triglia T, Maier AG, Cowman AF (2004) Transfection of the human malaria parasite *Plasmodium falciparum*. *Methods Mol Biol* **270:** 263–276

Craig A, Scherf A (2001) Molecules on the surface of the *Plasmodium falciparum* infected erythrocyte and their role in malaria pathogenesis and immune evasion. *Mol Biochem Parasitol* **115:** 129–143

Culvenor JG, Langford CJ, Crewther PE, Saint RB, Coppel RL, Kemp DJ, Anders RF, Brown GV (1987) *Plasmodium falciparum*: identification and localization of a knob protein antigen expressed by a cDNA clone. *Exp Parasitol* **63:** 58–67

Elmendorf HG, Haldar K (1993) Identification and localization of ERD2 in the malaria parasite *Plasmodium falciparum*: separation from sites of sphingomyelin synthesis and implications for organization of the Golgi. *EMBO J* **12:** 4763–4773

Elmendorf HG, Haldar K (1994) *Plasmodium falciparum* exports the Golgi marker sphingomyelin synthase into a tubovesicular network in the cytoplasm of mature erythrocytes. *J Cell Biol* **124:** 449–462

Fidock DA, Wellems TE (1997) Transformation with human dihydrofolate reductase renders malaria parasites insensitive to WR99210 but does not affect the intrinsic activity of proguanil. *Proc Natl Acad Sci USA* **94:** 10931–10936

Foth BJ, Ralph SA, Tonkin CJ, Struck NS, Fraunholz M, Roos DS, Cowman AF, McFadden GI (2003) Dissecting apicoplast targeting in the malaria parasite *Plasmodium falciparum*. *Science* **299:** 705–708

Gunther K, Tummler M, Arnold HH, Ridley R, Goman M, Scaife JG, Lingelbach K (1991) An exported protein of *Plasmodium falciparum* is synthesized as an integral membrane protein. *Mol Biochem Parasitol* **46:** 149–157

Haeggstrom M, Kironde F, Berzins K, Chen Q, Wahlgren M, Fernandez V (2004) Common trafficking pathway for variant antigens destined for the surface of the *Plasmodium falciparum*-infected erythrocyte. *Mol Biochem Parasitol* **133:** 1–14

Haldar K, Mohandas N, Samuel BU, Harrison T, Hiller NL, Akompong T, Cheresh P (2002) Protein and lipid trafficking induced in erythrocytes infected by malaria parasites. *Cell Microbiol* **4:** 383–395

Hiller NL, Bhattacharjee S, van Ooij C, Liolios K, Harrison T, Lopez-Estrano C, Haldar K (2004) A host-targeting signal in virulence proteins reveals a secretome in malarial infection. *Science* **306:** 1934–1937

Kara UA, Stenzel DJ, Ingram LT, Bushell GR, Lopez JA, Kidson C (1988) Inhibitory monoclonal antibody against a (myristylated) small-molecular-weight antigen from *Plasmodium falciparum* associated with the parasitophorous vacuole membrane. *Infect Immun* **56:** 903–909

Kaviratne M, Khan SM, Jarra W, Preiser PR (2002) Small variant STEVOR antigen is uniquely located within Maurer's clefts in *Plasmodium falciparum*-infected red blood cells. *Eukaryot Cell* **1:** 926–935

Kilejian A (1979) Characterization of a protein correlated with the production of knob-like protrusions on membranes of erythrocytes infected with *Plasmodium falciparum*. *Proc Natl Acad Sci USA* **76:** 4650–4653

Knuepfer E, Rug M, Klonis N, Tilley L, Cowman AF (2005) Trafficking of the major virulence factor to the surface of transfected *P. falciparum*-infected erythrocytes. *Blood* **105:** 4078–4087

Kriek N, Tilley L, Horrocks P, Pinches R, Elford BC, Ferguson DJ, Lingelbach K, Newbold CI (2003) Characterization of the pathway for transport of the cytoadherence-mediating protein, PfEMP1, to the host cell surface in malaria parasite-infected erythrocytes. *Mol Microbiol* **50:** 1215–1227

Lambros C, Vanderberg JP (1979) Synchronization of *Plasmodium falciparum* erythrocytic stages in culture. *J Parasitol* **65:** 418–420

Limpaiboon T, Shirley MW, Kemp DJ, Saul A (1991) 7H8/6, a multicopy DNA probe for distinguishing isolates of *Plasmodium falciparum*. *Mol Biochem Parasitol* **47:** 197–206

Lopez-Estrano C, Bhattacharjee S, Harrison T, Haldar K (2003) Cooperative domains define a unique host cell-targeting signal in *Plasmodium falciparum*-infected erythrocytes. *Proc Natl Acad Sci USA* **100:** 12402–12407

Marti M, Good RT, Rug M, Knuepfer E, Cowman AF (2004) Targeting malaria virulence and remodeling proteins to the host erythrocyte. *Science* **306:** 1930–1933

McRobert L, Preiser P, Sharp S, Jarra W, Kaviratne M, Taylor MC, Renia L, Sutherland CJ (2004) Distinct trafficking and localization of STEVOR proteins in three stages of the *Plasmodium falciparum* life cycle. *Infect Immun* **72:** 6597–6602

Miller LH, Baruch DI, Marsh K, Doumbo OK (2002) The pathogenic basis of malaria. *Nature* **415:** 673–679

Moller S, Croning MD, Apweiler R (2001) Evaluation of methods for the prediction of membrane spanning regions. *Bioinformatics* **17:** 646–653

Neupert W, Brunner M (2002) The protein import motor of mitochondria. *Nat Rev Mol Cell Biol* **3:** 555–565

Papakrivos J, Newbold CI, Lingelbach K (2005) A potential novel mechanism for the insertion of a membrane protein revealed by a biochemical analysis of the *Plasmodium falciparum* cytoadherence molecule PfEMP-1. *Mol Microbiol* **55:** 1272–1284

Pologe LG, Pavlovec A, Shio H, Ravetch JV (1987) Primary structure and subcellular localization of the knob-associated histidine-rich protein of *Plasmodium falciparum*. *Proc Natl Acad Sci USA* **84:** 7139–7143

Przyborski J, Lanzer M (2004) Parasitology. The malarial secretome. *Science* **306:** 1897–1898

Rudiger S, Germeroth L, Schneider-Mergener J, Bukau B (1997) Substrate specificity of the DnaK chaperone determined by screening cellulose-bound peptide libraries. *EMBO J* **16:** 1501–1507

Sam-Yellowe TY, Florens L, Johnson JR, Wang T, Drazba JA, Le Roch KG, Zhou Y, Batalov S, Carucci DJ, Winzeler EA, Yates III JR (2004) A *Plasmodium* gene family encoding Maurer's cleft membrane proteins: Structural properties and expression profiling. *Genome Res* **14:** 1052–1059

Soll J, Schleiff E (2004) Protein import into chloroplasts. *Nat Rev Mol Cell Biol* **5:** 198–208

Staalsoe T, Giha HA, Dodoo D, Theander TG, Hviid L (1999) Detection of antibodies to variant antigens on *Plasmodium falciparum*-infected erythrocytes by flow cytometry. *Cytometry* **35:** 329–336

Thompson JD, Higgins DG, Gibson TJ (1994) CLUSTAL W: improving the sensitivity of progressive multiple sequence alignment through sequence weighting, position-specific gap penalties and weight matrix choice. *Nucleic Acids Res* **22:** 4673–4680

Trager W, Jensen JB (1976) Human malaria parasites in continuous culture. *Science* **193:** 673–675

Vincensini L, Richert S, Blisnick T, Van Dorsselaer A, Leize-Wagner E, Rabilloud T, Braun Breton C (2005) Proteomic analysis identifies novel proteins of the Maurer's clefts, a secretory compartment delivering *Plasmodium falciparum* proteins to the surface of its host cell. *Mol Cell Proteomics* **4:** 582–593

Waller KL, Cooke BM, Nunomura W, Mohandas N, Coppel RL (1999) Mapping the binding domains involved in the interaction between the *Plasmodium falciparum* knob-associated histidine-rich protein (KAHRP) and the cytoadherence ligand *P. falciparum* erythrocyte membrane protein 1 (PfEMP1). *J Biol Chem* **274:** 23808–23813

Waller KL, Nunomura W, Cooke BM, Mohandas N, Coppel RL (2002) Mapping the domains of the cytoadherence ligand *Plasmodium falciparum* erythrocyte membrane protein 1 (PfEMP1) that bind to the knob-associated histidine-rich protein (KAHRP). *Mol Biochem Parasitol* **119:** 125–129

Waller RF, Reed MB, Cowman AF, McFadden GI (2000) Protein trafficking to the plastid of *Plasmodium falciparum* is via the secretory pathway. *EMBO J* **19:** 1794–1802

Wickert H, Gottler W, Krohne G, Lanzer M (2004) Maurer's cleft organization in the cytoplasm of *Plasmodium falciparum*-infected erythrocytes: new insights from three-dimensional reconstruction of serial ultrathin sections. *Eur J Cell Biol* **83:** 567–582

Wickert H, Rohrbach P, Scherer S, Krohne G, Lanzer M (2003a) A putative Sec23 homologue of *Plasmodium falciparum* is located in Maurer's clefts. *Mol Biochem Parasitol* **129:** 209–213

Wickert H, Wissing F, Andrews KT, Stich A, Krohne G, Lanzer M (2003b) Evidence for trafficking of PfEMP1 to the surface of *P. falciparum*-infected erythrocytes via a complex membrane network. *Eur J Cell Biol* **82:** 271–284

Wickham ME, Rug M, Ralph SA, Klonis N, McFadden GI, Tilley L, Cowman AF (2001) Trafficking and assembly of the cytoadherence complex in *Plasmodium falciparum*-infected human erythrocytes. *EMBO J* **20:** 5636–5649

Wiser MF, Lanners HN, Bafford RA, Favaloro JM (1997) A novel alternate secretory pathway for the export of *Plasmodium* proteins into the host erythrocyte. *Proc Natl Acad Sci USA* **94:** 9108–9113

World Health Organization (2000) WHO Expert Committee on Malaria. *World Health Organ Tech Rep Ser* **892:** i–v, 1–74